



Design, synthesis and biological evaluation of novel 5-((substituted quinolin-3-yl/1-naphthyl) methylene)-3-substituted imidazolidin-2,4-dione as HIV-1 fusion inhibitors

Tarek S. Ibrahim^{a,b,*}, Riham M. Bokhtia^{b,c}, Amany M.M. AL-Mahmoudy^b, Ehab S. Taher^d, Mohammed A. AlAwadh^a, Mohamed Elagawany^e, Eatedal H. Abdel-Aal^b, Siva Panda^c, Ahmed M. Gouda^f, Hany Z. Asfour^g, Nabil A. Alhakamy^h, Bahaa G.M. Youssif^{i,*}

^a Department of Pharmaceutical Chemistry, Faculty of Pharmacy, King Abdulaziz University, Jeddah 21589, Saudi Arabia

^b Department of Pharmaceutical Organic Chemistry, Faculty of Pharmacy, Zagazig University, Zagazig 44519, Egypt

^c Department of Chemistry and Physics, Augusta University, Augusta, GA 30912, USA

^d Department of Pharmaceutical Organic Chemistry, Faculty of Pharmacy, Al-Azhar University, Assiut 71524, Egypt

^e Department of Pharmaceutical Chemistry, Faculty of Pharmacy, Damanhour University, Damanhour, Egypt

^f Department of Medicinal Chemistry, Faculty of Pharmacy, Beni-Suef University, Beni-Suef 62514, Egypt

^g Department of Medical Microbiology and Parasitology, Faculty of Medicine, King Abdulaziz University, Jeddah 21589, Saudi Arabia

^h Department of Pharmaceutics, Faculty of Pharmacy, King Abdulaziz University, Jeddah 21589, Saudi Arabia

ⁱ Department of Pharmaceutical Organic Chemistry, Faculty of Pharmacy, Assiut University, Assiut 71526, Egypt

ARTICLE INFO

Keywords:

Imidazolidine-2,4-dione
Quinoline
HIV
Inhibitors
Gp41

ABSTRACT

A series of novel 5-(substituted quinolin-3-yl or 1-naphthyl)methylene)-3-substituted imidazolidin-2,4-dione **9–26** was designed and synthesized. The prepared compounds were identified using ¹H NMR, ¹³C NMR as well as elemental analyses. The inhibitory activity of **9–26** on HIV-1_{IIIB} replication in MT-2 cells was evaluated. Some derivatives showed good to excellent anti-HIV activities as compounds **13**, **18**, **19**, **20**, **22** and **23**. They showed EC₅₀ of 0.148, 0.460, 0.332, 0.50, 0.271 and 0.420 μM respectively being more potent than compound **I** (EC₅₀ = 0.70 μM) and **II** (EC₅₀ = 2.40 μM) as standards. The inhibitory activity of **9–26** on infected primary HIV-1 domain, 92US657 (clade B, R5) was investigated. All the tested compounds consistently inhibited infection of this virus with EC₅₀ from 0.520 to 11.857 μM. Results from SAR studies showed that substitution on **ring A** with 6/7/8-methyl group resulted in significant increase in the inhibitory activity against HIV-1_{IIIB} infection (5- > 300 times) compared to the unsubstituted analog **9**. The cytotoxicity of these compounds on MT-2 cells was tested and their CC₅₀ values ranged from 11 to 85 μM with selectivity indexes ranged from 0.53 to 166. The docking study revealed nice fitting of the new compounds into the hydrophobic pocket of HIV-1 gp41 and higher affinity than NB-64. Compound **13**, the most active in preventing HIV-1_{IIIB} infection, adopted a similar orientation to compound **IV**. Molecular docking analysis of the new compounds revealed hydrogen bonding interactions between the imidazolidine-2,4-dione ring and LY5574 which were missed in the weakly active derivatives.

1. Introduction

Acquired immunodeficiency syndrome (AIDS) is a universal health risk and is considered one of the foremost causes of death in many HIV-infected patients [1]. In addition to long-term use toxicity and high cost; drug resistance growth for many antiretroviral drugs in present use, particularly reverse transcriptase inhibitors (RTIs) and protease

inhibitors (PIs) resulted in the loss of cytotoxic activity of many anti-HIV therapies counting highly active antiretroviral therapy (HAART) [2–4]. Therefore, advances in drug design and modeling are urgently needed in order to develop new compounds with potent anti-HIV activity and new modes of action [5]. Attachment and insertion into the host cell membrane is the most important step for human immunodeficiency virus type 1 (HIV-1) to begin its life cycle through the

* Corresponding authors at: Pharmaceutical Chemistry, Faculty of Pharmacy, King Abdulaziz University, Jeddah 21589, Saudi Arabia. (T.S. Ibrahim). Pharmaceutical Organic Chemistry Department, Faculty of Pharmacy, Assiut University, Assiut 71526, Egypt. (B.G.M. Youssif).

E-mail addresses: tmabraham@kau.edu.sa (T.S. Ibrahim), bgyoussif@ju.edu.sa, bahaa.youssif@pharm.aun.edu.eg (B.G.M. Youssif).

<https://doi.org/10.1016/j.bioorg.2020.103782>

Received 29 December 2019; Received in revised form 19 February 2020; Accepted 19 March 2020

Available online 24 March 2020

0045-2068/ © 2020 Elsevier Inc. All rights reserved.

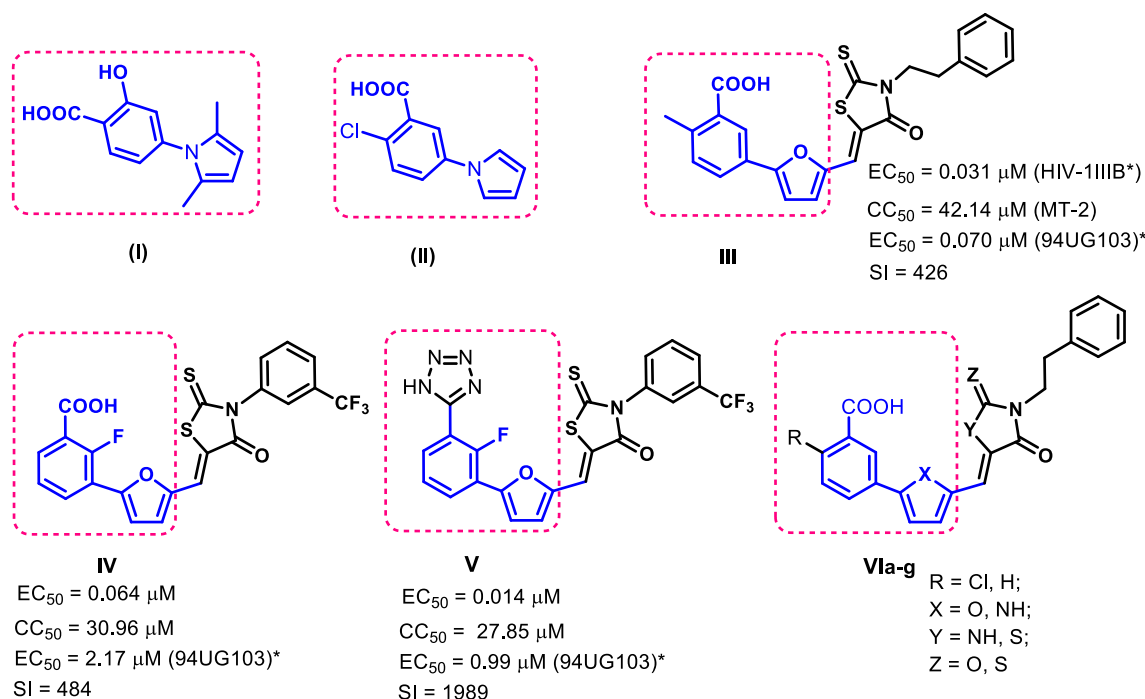


Fig. 1. Small molecules with HIV-1 gp41 inhibitory activities.

use of host cell machinery [6], thereby, development of new fusion inhibitors has been the focus of new drug discovery for many years [7–10]. Viral envelope binding glycoprotein (Env) surface subunit gp120 to cellular receptor CD4 and co-receptor CXCR4 or CCR5 initiates HIV-1 entry by activating a sets of conformational changes in the transmembrane subunit gp41 leading to formation of a six-helix bundle (6-HB) core and facilitating the fusion of membranes [11–13]. Three parallel *N*-terminal heptad repeat units (NHR) frequently form an internal trimeric coiled coil, and three C-terminal heptad repeat units (CHR) are then packed into the hydrophobic grooves retained on the central trimeric core in an anti-parallel manner [14–17]. A deep hydrophobic cavity in the groove substantially establishes the 6-HB and serves as an attractive base for the development of small molecule HIV fusion/entry inhibitors [18]. Previously, *N*-substituted pyrrole derivatives (I) and (II) (NB-2 and NB-64) were reported [19] as small molecules with low micromolar inhibitory action against HIV-1 infection, HIV-1 Env-mediated cell-cell fusion and gp41 six-helix bundles, Fig. 1. Docking studies showed that both (I) and (II) bind on the gp41 NHR-trimer to the deep hydrophobic cavity, but only fill a portion of the pocket space [19]. Later on, Katritzky *et al.* have reported a series of 2-aryl-5-(4-oxo-3-phenethyl-2-thioxothiazolidin-ylidene methyl)furan derivatives [20] with anti-HIV-1 activity. The new derivatives exhibited higher anti-HIV-1 activity than (I) and (II). This could be suggested that the highly bulky molecule may occupy more space in the hydrophobic cavity, and consequently, higher binding activity and stronger inhibitory activity on 6-HB formation [20]. Among these derivatives, compound III was the most selective ($\text{SI} = 426$), Fig. 1.

Jiang *et al.* have also reported two series of 5-((aryl-furan/1*H*-pyrrol-2-yl)methylene)-2-thioxo-3-(3-(trifluoromethyl)phenyl)-thiazolidin-4-ones which showed effective inhibition of HIV-1 infection [21]. Among these derivatives, compound IV blocked gp41 six-helix bundle formation and HIV-1 mediated cell-cell fusion, Fig. 1. Replacement of the carboxylic group in compound IV with the isosteric tetrazole ring (Compound V) resulted in significant increase in the anti-HIV-1_{III^B} activity ($\text{EC}_{50} = 0.014 \mu\text{M}$) with slight increase in cytotoxicity against

MT-2 cells ($\text{CC}_{50} = 27.85 \mu\text{M}$). Accordingly, the tetrazolyl analog V exhibited a selectivity index (SI) of 1989 compared to 484 for the parent IV. Replacement of the furan oxygen by NH group resulted in decrease in both anti-HIV-1_{III^B} activity ($\text{EC}_{50} = 0.615 \mu\text{M}$) and selectivity ($\text{SI} = 48$) to one-tenth of the parent IV [21]. Jiang *et al.* also have reported another 2,5-disubstituted furans/pyrroles series with higher anti-HIV-1 activity than (I) and (II) [22]. Among these derivatives, compound VI displayed significant inhibition against HIV-1_{III^B} infection [22]. Mechanistic study revealed the ability of compound VI to block gp41 six-helix bundle formation. Although carboxylic acid group seems to be important for the binding to gp41, several nonacidic compounds were reported as HIV-1 gp41 fusion inhibitors. Among these inhibitors which lack the carboxylic acid group, SB-H02, compound VII (Fig. 2) showed HIV-1 inhibitory activity with IC_{50} of $13.3 \mu\text{M}$ [10]. In addition, Frey *et al.* have developed a protein-based assay to screen the ability of small molecules to inhibit the formation of post fusion gp41 [23]. They have screened several library including 34800 small organic compounds for their ability to inhibit HIV infection. Among the tested compounds, four compounds have displayed the most promising results. Of these compounds 5M038 VIII and S2986 IX exhibited envelop-mediated membrane fusion in viral infectivity and cell-cell fusion assay, Fig. 2. DAA-9 X was identified through a docking protocol as potential gp41 fusion inhibitor [24]. Docking results of DAA-9 revealed binding affinity to gp41 comparable to that of NB-64 (II). Moreover, DAA-9 also showed *in vitro* anti-HIV-1 activity comparable to that of NB-64.

1.1. Rational and design

Compounds IV and V were reported among a series of 4-thiazolidinone-based derivatives that 6-target HB formation in HIV-1 gp41 [21]. Molecular docking analysis of this series revealed the importance of the salt-bridge, hydrophobic, and hydrogen bond-forming groups in their structures for inhibition of 6-HB formation. However, evaluation of drug-likeness parameters of compounds IV and V revealed high

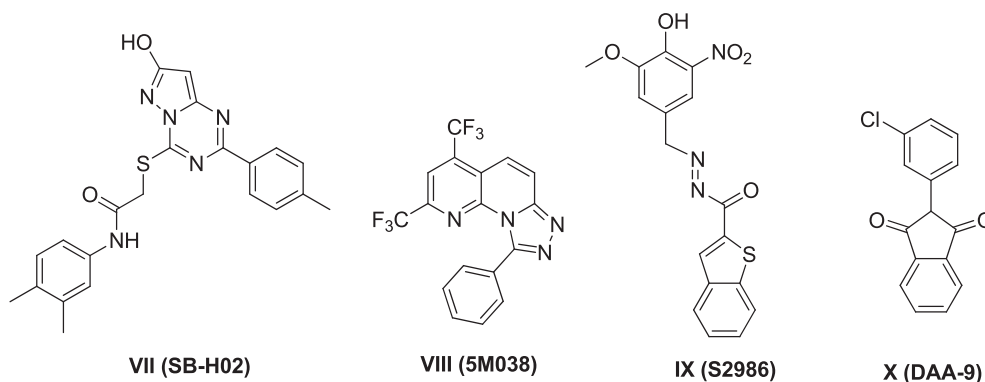


Fig. 2. HIV-1 gp41 fusion inhibitors lacking the carboxylic acid group.

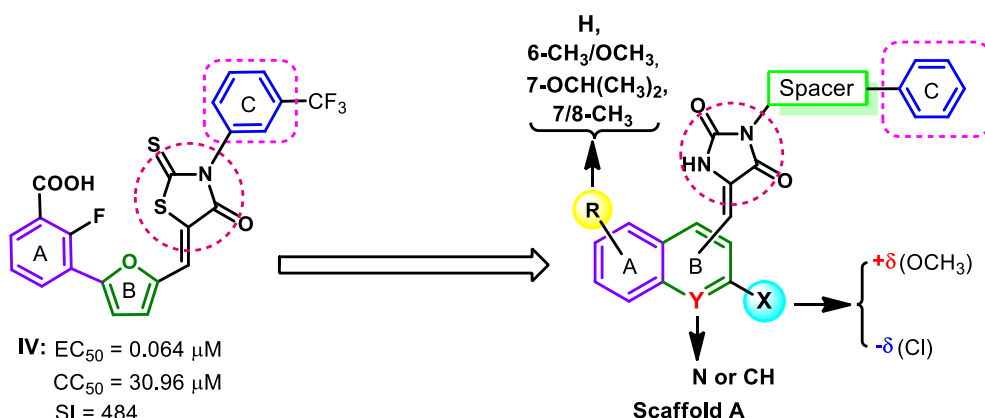


Fig. 3. Rational design and structural modification of scaffold A.

lipophilicity (ClogP > 5), high molecular weight (> 500), low drug-likeness score and 1–2 violations from Lipinski, Ghose, Egan and Muegge rules (Supplementary data, Tables S1 and S2, Figs. S1 and S2). Moreover, the presence of carboxylic acid group seems to be not essential for the anti-HIV activity of compounds VII–X. accordingly, the aim of the present study was to manipulate the chemical structure of compound IV to obtain new potent antiviral agents, lacking the carboxylic acid group.

Scaffold A (Fig. 3) was designed by isosteric replacement of the two sulfur atoms in compound IV with the more polar groups (O and NH) which can bind to the hydrophobic pocket of HIV-1 GP41 protein through hydrogen bonding interactions, Fig. 3. In addition, the 2-fluoro-3-(furan-2-yl)benzoic acid moiety in compound IV was replaced with quinoline nucleus, substituted with various hydrophobic substituents (CH₃, OCH₃, OCH(CH₃)₂) that can interact hydrophobically with the hydrophobic residues in GP41. Position 2 of the quinoline nucleus was substituted with either electron-donating/withdrawing groups to evaluate the impact of their electronic effects on the activity of the new compounds. The length of the spacer in scaffold A was increased to two carbon atoms to extend the hydrophobic scaffold and increase molecular volume of the new compounds which allow them to occupy larger volumes of the hydrophobic pocket. A preliminary evaluation of physicochemical properties of the prototype derivative (9) of scaffold A revealed an improvement in physicochemical properties and drug-likeness score (Supplementary data, Tables S3 and S4, Fig. S3).

The synthesis of newly designed compounds was done by Knoevenagel condensation reaction between 3-substituted imidazolidine-2,4-dione **3a,b** [25] and either substituted quinolin-3-aldehyde (**6a-g** and **7a-d**) [26] or 1-naphthaldehyde (**8**) in presence

of TMP as a base. The prepared compounds were identified using ¹H NMR, ¹³C NMR as well as elemental analyses. The inhibitory activity of **9–26** on HIV-1_{IIIB} replication was evaluated using an p24 measurement enzyme-linked immunosorbent assay (ELISA) in MT-2 cells against (**I**) and (**II**) (NB-2 and NB-64) as the reference compounds.

2 Results and discussion

2.1 Chemistry

Synthesis of **9–26** having 5-((substituted quinolin-3-yl or 1-naphthyl)methylene)-3-substituted imidazolidine-2,4-diones was outlined in Scheme 1. Imidazolidine-2,4-dione **1** was reacted with (2-bromoethyl) benzene or benzyl bromide in dimethylformamide to afford 3-Substituted imidazolidine-2,4-dione **3a-b** [25]. Refluxing of **3a-b** with substituted quinolin-3-aldehyde [26] **6a-g** and **7a-d** or 1-naphthaldehyde **8** derivatives in the presence of TMP in ethanol to yield the desired target products **9–26**. As a representative example of this series, the ¹H NMR spectrum of **24** demonstrated the presence of a signal at 10.95 ppm of NH, two sets of C₈-H and C₆-H of quinoline doublets at 7.70 and 7.40 ppm with $J = 2.5$ Hz each, two signals with one and six protons integration at 3.24 (s) and 165–1.61 (m) ppm attributed to isopropyl group and olefinic proton signal at δ 6.40 (s) as well as aromatic protons. The ¹³C NMR spectrum of compound **24** showed two signals at 162.8 and 157.9 ppm assigned to the ketonic carbonyls of imidazolidine-2,4-dione and all other carbons appear at their expected chemical shifts. In addition, data from the elemental analysis further confirmed the assigned structure.

Comp	R	X	n	Comp	R	X	n
9	H	Cl	1	17	7-CH ₃	Cl	2
10	6-CH ₃	Cl	1	18	7-OCH ₃	Cl	2
11	6-OCH ₃	Cl	1	19	7-OCH(CH ₃) ₂	Cl	2
12	7-CH ₃	Cl	1	20	8-CH ₃	Cl	2
13	8-CH ₃	Cl	1	21	H	OCH ₃	1
14	H	Cl	2	22	6-OCH ₃	OCH ₃	1
15	6-CH ₃	Cl	2	23	H	OCH ₃	2
16	6-OCH ₃	Cl	2	24	6-OCH ₃	OCH ₃	2

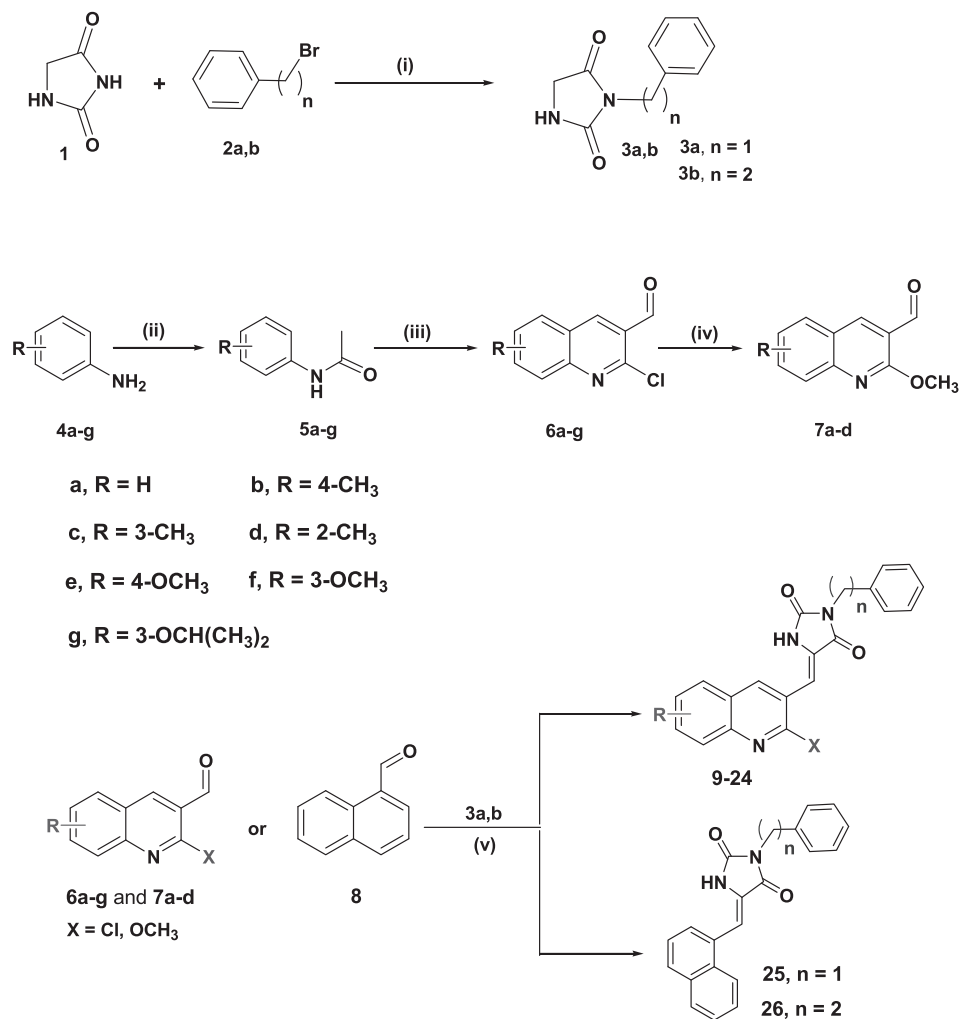
2.2. Biological activities

2.2.1. HIV-1 inhibitory activity

p24 ELISA assay was used to test the inhibitory effect of **9–26** on HIV-1 III_B replication in MT-2 cells [27] using **I** and **II** as the reference compounds, Table 1. Most of the compounds tested substantially inhibited dose-dependent replication of HIV-1 III_B. Generally, 5-((substituted-quinolin-3-yl)methylene)-3-substituted imidazolidin-2,4-dione derivatives **9–24** showed superior inhibitory activity compared to their naphthyl counterparts **25** and **26**, Table 1. The best compounds against HIV-1 III_B are **13**, **18**, **19**, **20**, **22** and **23**, which showed EC₅₀ of 0.148,

0.460, 0.332, 0.50, 0.271 and 0.420 μ M respectively being more potent than compound **I** (EC₅₀ = 0.70 μ M) and **II** (EC₅₀ = 2.40 μ M) but less potent than compound **IV** (EC₅₀ = 0.064 μ M) as standards. The 3-benzyl-5-((2-chloro-8-methylquinolin-3-yl)methylene) derivative **13** (R = 8-Me, X = Cl and n = 1) was the most effective of the synthesized derivatives with an EC₅₀ value of 0.148 μ M against MT-2 cell. The unsubstituted derivative **9** (R = H) was about 348 folds less potent than **13** showing EC₅₀ 50.61 μ M. Replacement of the 8-Me group in compound **13** by 6-methyl or 6-OMe or even 7-Me in compounds **10**, **11** and **12** respectively resulted in a reduction in the EC₅₀ value of a least 5 folds, indicating the importance of the 8-methyl group for HIV-1 III_B replication in MT-2 cell inhibitory activity. Moreover, the 5-((2-chloro-8-methylquinolin-3-yl)methylene)-3-phenethyl derivative **20** (R = 8-Me, X = Cl and n = 2) was less potent than **13** suggesting the importance of the N-benzylimidazolidine-2,4-dione architecture for the inhibitory activity. It should be noted that compounds **21–24** with 2-OMe in the quinoline ring were more active than their 2-Cl congeners **9**, **11**, **14** and **16** respectively.

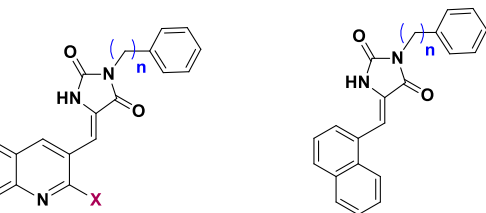
The **9–26** inhibitory effect on primary HIV-1 isolate, 92US657 (class B, R5), as class B is the most prevalent subtype in the United States, has been determined. All the compounds examined reliably inhibited HIV-1 92US657 isolate infection with EC₅₀ between 0.520 and 11.857 μ M,



Reagents and conditions: (i) DMF, K₂CO₃, 80 °C, overnight; (ii) Ac₂O, AcOH, rt, 1h; (iii) DMF, POCl₃, 70 °C, 18h; (iv) NaOMe, EtOH, 40 °C, 3–6h; (v) EtOH, TMP, reflux, 72h.

Scheme 1. Synthetic route of novel (Z)-5-((substituted quinolin-3-yl or 1-naphthyl)methylene)-3-substituted imidazolidine-2,4-diones **9–26**. **Reagents and conditions:** (i) DMF, K₂CO₃, 80 °C, overnight; (ii) Ac₂O, AcOH, rt, 1 h; (iii) DMF, POCl₃, 70 °C, 18 h; (iv) NaOMe, EtOH, 40 °C, 3–6 h; (v) EtOH, TMP, reflux, 72 h.

Table 1
Anti-HIV-1_{IIIb} Activity, Cytotoxicity and Selectivity Indexes of compounds 9–26.



Compound	EC ₅₀ ^a (μM)	CC ₅₀ ^b (μM)	SI ^c	EC ₅₀ ^d (μM)
9	50.61 ± 0.01	26.91 ± 1.80	0.53	1.66 ± 0.21
10	5.54 ± 0.01	56.23 ± 1.23	10.15	1.16 ± 0.02
11	1.96 ± 0.004	97.26 ± 5.36	49.62	0.70 ± 0.12
12	0.72 ± 0.007	41.68 ± 1.16	57.88	10.86 ± 1.29
13	0.148 ± 0.006	17.37 ± 0.99	117.36	8.70 ± 2.14
14	2.92 ± 0.004	85.43 ± 4.66	29.25	1.05 ± 0.11
15	22.76 ± 0.002	58.88 ± 4.23	2.58	0.52 ± 0.04
16	1.01 ± 0.01	19.05 ± 0.57	18.86	1.23 ± 0.24
17	2.55 ± 0.004	14.12 ± 1.66	5.54	1.004 ± 0.003
18	0.46 ± 0.002	32.36 ± 2.47	70.34	1.05 ± 0.01
19	0.33 ± 0.001	54.95 ± 4.31	166.50	11.85 ± 3.24
20	0.50 ± 0.004	43.51 ± 6.22	87.02	1.32 ± 0.41
21	1.41 ± 0.008	11.22 ± 2.13	7.95	2.49 ± 0.45
22	0.27 ± 0.003	42.65 ± 6.33	157.96	0.75 ± 0.12
23	0.42 ± 0.002	43.65 ± 6.74	103.92	6.87 ± 0.22
24	1.51 ± 0.002	28.84 ± 5.49	19.09	1.42 ± 0.11
25	1.52 ± 0.004	35.48 ± 6.39	23.34	2.80 ± 0.61
26	1.93 ± 0.005	19.05 ± 3.94	9.87	1.39 ± 0.42
NB-2 (I)	0.70 ± 0.002	133.4 ± 5.42	191	–
NB-64 (II)	2.4 ± 0.008	335.7 ± 6.68	140	–
Compound IV ^e	0.064	30.96	484	–

^a EC₅₀ to prevent of HIV-1_{IIIb} infection. Each compound has been measured in triplicates and the data is shown as the mean ± SD.

^b CC₅₀ for MT-2 cells.

^c SI was determined to inhibit HIV-1_{IIIb} infection on the basis of CC₅₀ for MT-2 cells and EC₅₀.

^d Primary HIV-1 Isolate inhibitory function, 92US657 (R5, Class B).

^e All data have been obtained from previous publication [21] for comparison purposes.

Table 1. The best inhibitory activity was shown by Compound 15. **Table 1** results showed that the newly synthesized 9–26 compounds are effective against both laboratory and primary HIV-1 strains.

2.2.2. Detection of in vitro cytotoxicity

A colorimetric XTT assay [28] was used to determine the cytotoxicity of 9–26 on MT-2 cells. Their CC₅₀ (50% cytotoxicity concentration) ranged from 11 to 85 μM and their selectivity index ranged from 0.53 to 166 (**Table 1**). Two of the best HIV-1 _{IIIb} inhibitors are 13 and 19 with EC₅₀ of 0.148 and 0.33 μM and SI of 117 and 166 in comparison to compound IV (SI = 484).

2.2.3. Structure activity relationship (SAR)

The impact of different substituents in compounds 9–26 on both anti-HIV-1 inhibitory activity and selectivity was evaluated in this section based on the biological results, **Table 1**. Based on these results, compound 13 exhibited the highest inhibitory activity against HIV-1 infection. Removal of the 8-methyl group in compound 13 resulted in sharp decrease in both inhibitory activity and selectivity against HIV-1 as indicated by the results of compound 9. Moreover, the other hand, replacement of the 8-methyl-2-chloro-quinoline by 1-naphthalenyl resulted in 10 times decrease in activity and 2 times decrease in selectivity against HIV-1, **Fig. 4**.

The movement of the 8-methyl group in compound 13 or C6 or C7 (compounds 10 and 12) resulted also in reduction in the activity and selectivity toward HIV-1, where compound 10 was less active than

compound 12. However, a slight increase in anti-HIV-1 activity and a significant increase in selectivity was observed on replacement of the 6-methyl group in compound 10 by methoxy group. In addition, increasing the length of the spacer between the phenyl and the imidazolidine ring by one carbon resulted in reduction of the inhibitory activity and selectivity against HIV-1. The resulting compound 20 was more than three times less potent than compound 13. The removal of the 8-methoxy group in compound 20 decreased both activity and selectivity against HIV-1. The 8-desmethoxy analog 14 (EC₅₀ = 2.92 μM, SI = 29.25) was nearly 6 times less potent than compound 20, **Fig. 4**.

An increase in activity of compound 14 was observed on replace of the 2-Cl by OCH₃ group. Moreover, substitution on quinoline ring of compound 14 by 7-OCH₃, 7-OCH(CH₃)₂, or 8-CH₃ also resulted in increase in activity (EC₅₀ = 0.33–0.5 μM) and selectivity (SI = 70.34–166.50) where compound 19 was the most selective among all the new compounds, **Fig. 4**.

2.3. Docking study into HIV-1 gp41

In the last two decades, several small molecules were reported as HIV-1 fusion inhibitors [21,29,30]. The ability of these compounds to interfere with the six-helix bundle (6-HB) formation was evaluated in several reports [21,29,30]. Of these inhibitors, the reference compound IV was reported among a series of 4-thiazolidinone-based derivatives that target HIV-1 gp41 and inhibit 6-HB formation [21]. The results of the docking study of these compounds into the hydrophobic pocket of HIV-1 gp41 revealed a noticeable correlation with the experimental results [21].

In this work, a molecular docking study was performed to evaluate binding affinities, modes, and interactions of compounds 9–26 hydrophobic pocket of HIV-1 gp41. The study was performed considering the previously reported docking protocols [21,31]. The study was performed using AutoDock 4.2 [32]. The core structure of HIV-1 gp41 (PDB code: 1AIK) [15] was obtained from the protein data bank (<https://www.rcsb.org/>). Ligands, protein, grid parameter, and docking parameter files were prepared according to the previous reports [31,33–36]. Validation of the docking results was done by comparing the binding modes and interactions of compounds IV and NB-64 (II) with those in the previous reports [21,31]. discovery studio visualizer [37] was used to generate the 2/3D binding modes of the new compound. The results of this study were represented in **Figs. 5–8**.

The results of the docking study revealed nice fitting of compounds IV and NB-64 (II) into the hydrophobic pocket of HIV-1 gp41 protein. Molecular docking analyses of compound IV and NB-64 (II) revealed the formation of an important salt-bridge interaction with LYS574. Moreover, the two compounds exhibited different types of hydrophobic interactions with the key amino acids (GLN567, LEU568, VAL570, TRP571, LYS574, GLN575, and TRP631) in the hydrophobic pocket. The 2D binding modes of compounds IV and NB-64 (II) showing different types of interactions were provided in **Fig. 5**.

The new compounds 9–26 exhibited higher affinities (ΔG_b = –6.06 to –6.93 kcal/mol) compared to NB-64 (ΔG_b = –4.89 kcal/mol for). The higher affinities of the new compounds could be attributed to their extended hydrophobic scaffold which allowed them to interact more hydrophobically with amino acids in the hydrophobic pocket. The large molecular volumes of the new compounds allowed them also to occupy more space in the hydrophobic pocket. On the other hand, the lower affinities of the new compounds compared to compound IV (ΔG_b = –7.02 kcal/mol) could be attributed to the absence of the salt-bridge with LYS574.

The relationship between docking results of the new compounds 9–26 and their biological data (**Table 1**), could be explained on the basis of their binding affinities, orientations, and types of interactions into the hydrophobic pocket in comparison with compounds II and reference IV. Molecular docking analyses of the best-fit conformations of the new compounds revealed different orientations of the new

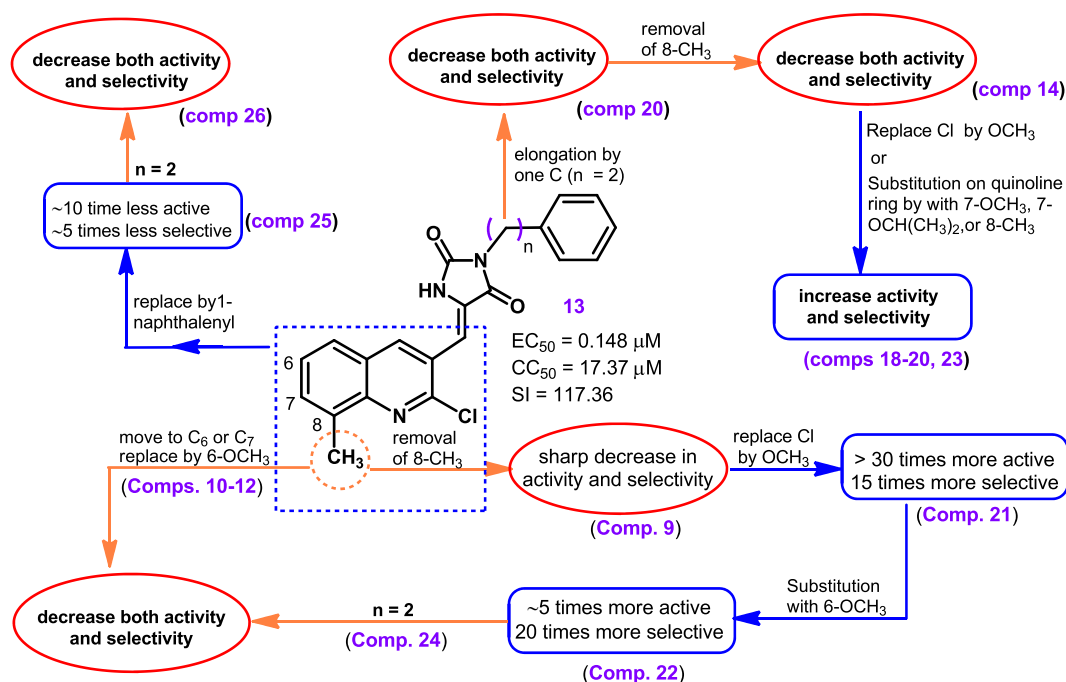


Fig. 4. SAR of the anti-HIV-1_{III}B activity and selectivity of compounds 9–26.

compounds from compound IV, Fig. 6. Compounds 12, 13, 16 and 23 (EC₅₀ values ≤ 1) adopted a quite similar orientation to compound IV. Among these four compounds, compound 13 was most active (EC₅₀ = 0.148) and exhibited the highest affinity. On the other hand, compounds 9, 10, 15, 17 and 26 which have weakest antiviral activity (EC₅₀ values = 1.93–50.61 μM) exhibited different orientations from that of compound IV.

Compound 13, the most active in preventing HIV-1_{III}B infection, exhibited a binding affinity of −6.84 kcal/mol which was higher than that NB-64 and comparable to compound IV. These results were in concordance with the EC₅₀ values of these three compounds (II, IV, and 13), Table 1. Moreover, the best-fit conformation of compound 13 adopted an orientation similar to compound IV, Fig. 7. This orientation allowed the two oxygen atoms of the imidazolidine-2,4-dione ring in compound 13 to form a cluster of hydrogen bonds with LYS574 and GLN575. These hydrogen bonds could compensate for the absence of the salt-bridge observed with compounds II and IV. These hydrogen bonds, together with the high affinity and orientation of compound 13 could account for its highest antiviral activity.

Moreover, compound 22, the second most active compound in

preventing HIV-1_{III}B infection (EC₅₀ = 0.27 μM), exhibited also higher binding free energy than that of NB-64, but lower than those of compound IV and 13. These results were also matched with the EC₅₀ values of these compounds, Table 1. However, the molecular docking analysis of compound 22 revealed a different orientation from compounds IV and 13 which could account for the observed decrease in the antiviral activity of compound 22 compared to compounds IV and 13. However, the orientation of compound 22 was still able to form two hydrogen bonds with key amino acids, LYS574 and GLN575, Fig. 7.

In addition, compounds 18, 19 and 23 exhibited nearly equal binding affinities toward the hydrophobic pocket (ΔG_b = −6.06 to −6.19 kcal/mol). These results were quite matched with the biological results of the three compounds (EC₅₀ values = 0.33–0.46 M). Among these compounds, compound 19 displayed the highest affinity and antiviral activity, Table 1. Moreover, compounds 21 and 25 exhibited nearly equal binding affinities toward the hydrophobic pocket and displayed similar antiviral activity with EC₅₀ values of 1.41 and 1.52 μM, respectively.

On the other hand, compound 26 exhibited higher binding affinity than compound 13. However, compound 26 was about ten times less

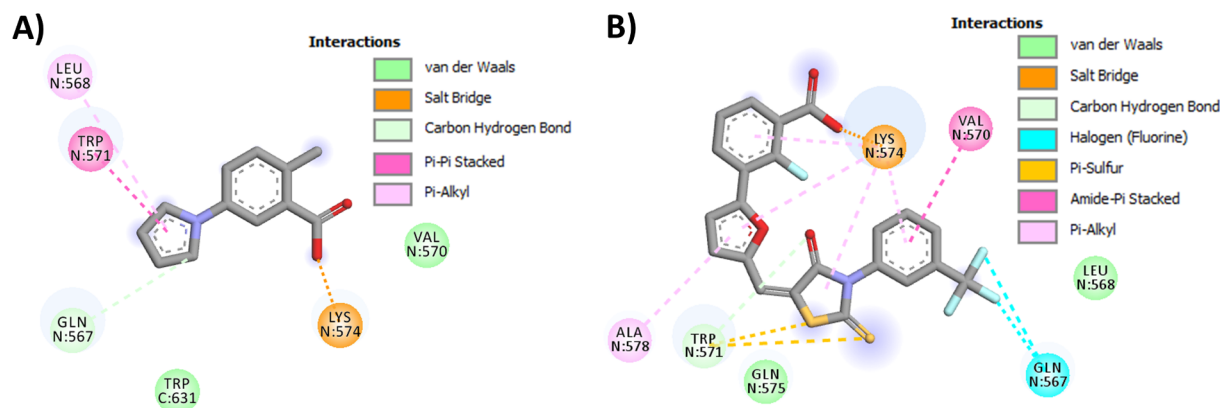


Fig. 5. Binding interactions of compounds IV and II into the hydrophobic pocket of HIV-1 gp41 protein (PDB: 1A1K) A) 2D binding mode of compound II; B) 2D binding mode of compound IV, showing one salt bridge with LYS574 and different types of hydrophobic interactions, hydrogen atoms were omitted for clarity.

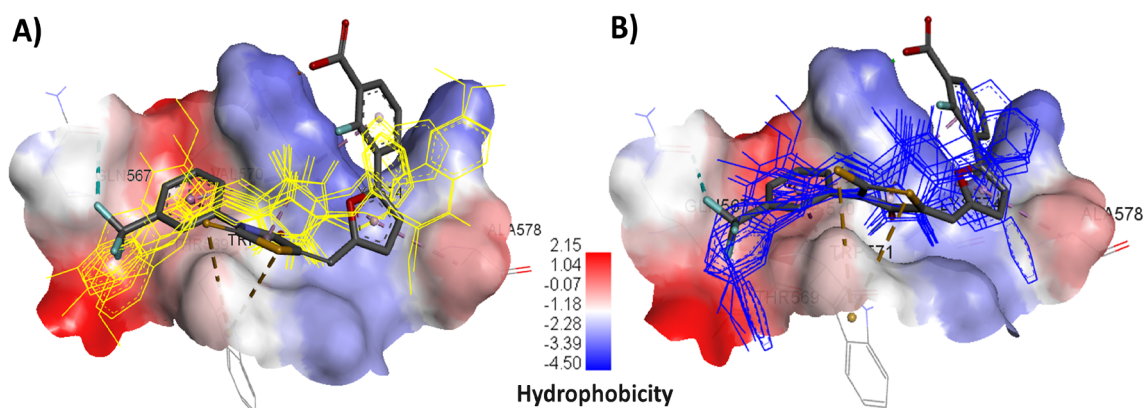


Fig. 6. The new compounds 9–24 overlaid with compound IV: A) Overlay of the best fit conformation of compounds 9–13, 21 and 22 ($n = 1$, shown as yellow lines) with compound IV (shown as sticks colored by element); B) Overlay of the best fit conformation of compounds 14–20, 23, 24 ($n = 2$, shown as blue lines) with compound IV (shown as sticks colored by element). Receptor is shown as hydrophobicity surface; hydrogen atoms were omitted for clarity. (For interpretation of the references to colour in this figure legend, the reader is referred to the web version of this article.)

active than compound 13, Table 1. The molecular docking analysis of compound 26 revealed a different orientation from that of compound IV and 13. This orientation prevented the formation of the critical hydrogen bonds with LYS574 which could account for the weak antiviral activity of compound 26. In addition, investigation of the binding interactions of this compound revealed the presence of one unfavorable acceptor-acceptor interaction with the imidazolidine-2,4-dione oxygen, Fig. 8.

Similarly, compounds 9, 10, 15 and 17, the least active in preventing HIV-1_{IIIB} infection (Table 1), adopted different orientations from compounds IV and 13 and missed the hydrogen bonding interactions with LYS574.

3. Conclusion

In this study, a series of 5-((substituted quinolin-3-yl/1-naphthyl)methylene)-3-substituted imidazolidine-2,4-diones derivatives 9–26 were designed and synthesized. Spectral and elemental analyses confirmed the chemical structure of the new compounds. The ability of 9–26 to inhibit HIV-1_{IIIB} replication in MT-2 was assessed using a p24 ELISA assay. Cytotoxicity of these compounds against MT-2 cells was also evaluated. The results revealed the ability of most of the new compounds to significantly inhibit HIV-1_{IIIB} replication in a dose-dependent manner. Among the new derivatives, compound 13 was the most potent in inhibiting the HIV-1_{IIIB} infection with EC_{50} value of 0.148 μ M and selectivity index of 117.36. compound 13 exhibited EC_{50} value of 8.7 μ M against the primary HIV-1 Isolate, 92US657 (R5, Clade

B). SAR study revealed a significant increase in anti-HIV-1 activity and selectivity of the parent compound 9 was observed on elongation of the spacer between phenyl and imidazolidine rings from one to two carbons. Moreover, substitution with 7-methoxy group on the quinoline ring resulted in significant increase in the anti-HIV-1 activity and selectivity. In addition, replacement of the 2-chloro group in compounds 9, 11, 14 and 15 with methoxy resulted in increased activity and selectivity. The results of the docking study of the new compounds revealed nice fitting into the hydrophobic pocket of HIV-1 gp41. Due to their extended hydrophobic scaffold, all the new compounds 9–26 exhibited higher affinities than NB-64. Compound 13, the most active in preventing HIV-1_{IIIB} infection, adopted a similar orientation to compound IV and exhibited a comparable affinity. Molecular docking analysis of the new compounds revealed hydrogen bonding interactions between imidazolidine-2,4-dione ring of the new compounds and LYS574. These interactions were missed in most of the weakly active derivatives 9, 10, 15, 17 and 26.

4. Experimental

4.1. Chemistry

4.1.1. General details [See Appendix A]

4.1.1.1. General method for synthesis of (Z)-5-((substituted quinolin-3-yl or 1-naphthyl)methylene)-3-substituted imidazolidine-2,4-dione (9–26). A mixture of 2,6,7,8-tetrasubstituted quinolin-3-aldehyde 6a–g and 7a–d (2.5 mmol) or 1-naphthaldehyde 8 (2.5 mmol), 3-substituted

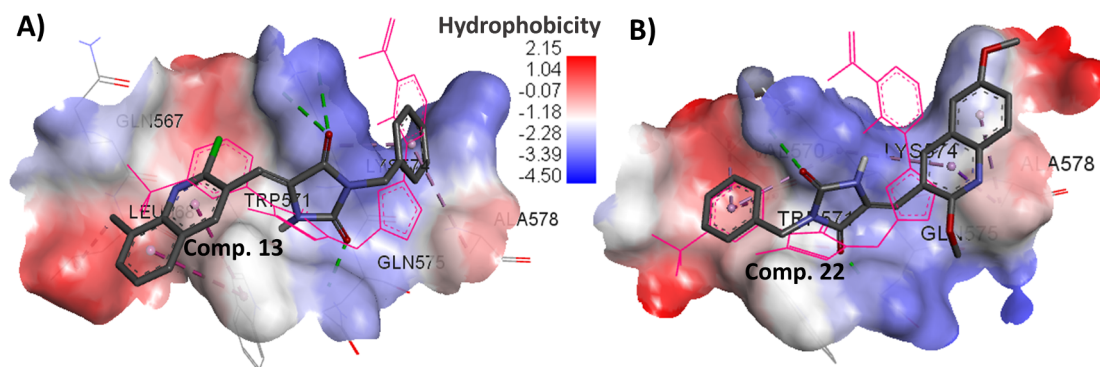


Fig. 7. Binding modes/interactions of compound 13 and 22 into the hydrophobic pocket of HIV-1 gp41 protein: A) 3D binding mode of compound 13 (shown as sticks colored by element) overlaid with compound IV (shown as pink lines); B) 3D binding mode of compound 22 (shown as sticks colored by element) overlaid with compound IV (shown as pink lines), hydrogen atoms were omitted for clarity. (For interpretation of the references to colour in this figure legend, the reader is referred to the web version of this article.)

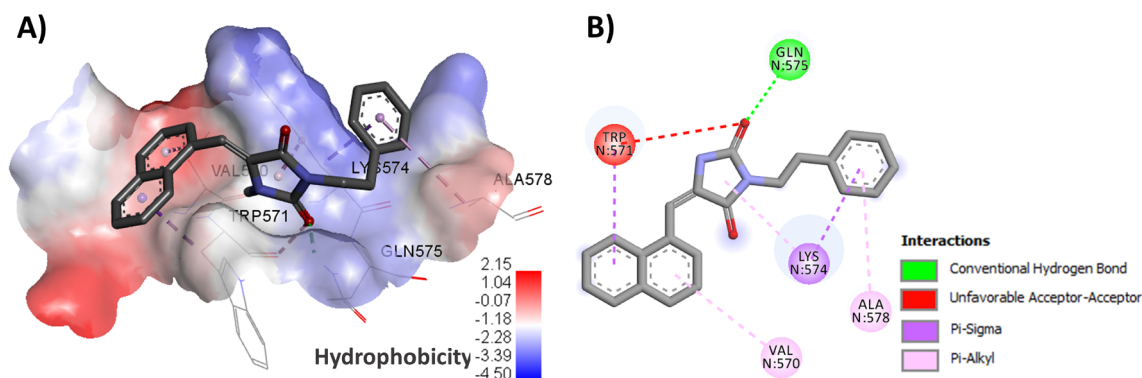


Fig. 8. Binding modes of compound **26** into the hydrophobic pocket of HIV-1 gp41 protein: A) 3D binding mode, receptor is shown as hydrophobicity surface; B) 2D binding mode of compound **26** (shown as sticks colored by element), hydrogen atoms were omitted for clarity.

imidazolidin-2,4-dione **3a,b** (0.5 g, 2.5 mmol) and 2–5 drops of 2,2,6,6-tetramethyl piperidine in 7 ml ethanol was heated under reflux for 72 h. After cooling the solid obtained was filtered and washed with cold ethanol to give compounds **9–26**.

4.1.1.1.1. (Z)-3-benzyl-5-((2-chloroquinolin-3-yl)methylene)imidazolidine-2,4-dione (9). Yellow crystals from ethanol, yield: 56% (0.54 g), m.p: 203–205 °C, ^1H NMR (500 MHz, DMSO- d_6) δ : 11.03 (s, 1H, NH, D $_2$ O exchangeable), 8.35 (s, 1H, C $_4$ -H of quinoline), 7.66 (d, J = 7.5 Hz, 2H, C $_{5,8}$ -H of quinoline), 7.53 (t, J = 8.0, 7.0 Hz, 2H, C $_{6,7}$ -H of quinoline), 7.36–7.21 (m, 5H, ArH), 6.68 (s, 1H, olefinic CH=C), 4.68 (s, 2H, CH $_2$); ^{13}C NMR (125 MHz, DMSO- d_6) δ : 163.6, 161.0, 154.1, 140.0, 138.2, 136.4, 131.2, 128.6, 128.4, 127.5, 127.4, 124.9, 122.5, 119.4, 115.1, 104.0, 41.4. Anal. Calcd. for C $_{20}$ H $_{14}$ ClN $_3$ O $_2$: C, 66.03; H, 3.88; N, 11.55. Found: C, 66.36; H, 4.12; N 11.83.

4.1.1.1.2. (Z)-3-benzyl-5-((2-chloro-6-methylquinolin-3-yl)methylene)imidazolidine-2,4-dione (10). Fine yellow crystals from ethanol, yield: 36% (0.36 g), m.p: 217–219 °C, IR: ν_{max} /cm $^{-1}$: 3468 (OH), 3104 (NH), 3021 (CH, aromatic), 2921, 2853 (CH, aliphatic), 1706 (C=O), 1591 (C=N), 1453 (C=C), 1182 (C-O), 700 (C-Cl); ^1H NMR (500 MHz, DMSO- d_6) δ : 8.45 (s, 1H, C $_4$ -H of quinoline), 7.93–7.85 (m, 2H, C $_{5,8}$ -H of quinoline), 7.65 (d, J = 8.5 Hz, 1H, C $_7$ -H of quinoline), 7.32–7.25 (m, 5H, ArH), 6.32 (s, 1H, NH, D $_2$ O exchangeable), 4.63–4.60 (m, H, olefinic CH=C), 4.54–4.51 (m, 2H, CH $_2$), 2.49 (s, 3H, CH $_3$); ^{13}C NMR (125 MHz, DMSO- d_6) δ : 172.3, 157.3, 146.4, 145.1, 137.8, 136.9, 136.6, 132.7, 132.6, 128.3, 127.3, 127.2, 127.1, 127.0, 60.5, 21.1. Anal. Calcd. for C $_{21}$ H $_{16}$ ClN $_3$ O $_2$: C, 66.76; H, 4.27; N, 11.72. Found: C, 67.00; H, 4.36; N 11.92.

4.1.1.1.3. (Z)-3-benzyl-5-((2-chloro-6-methoxyquinolin-3-yl)methylene)imidazolidine-2,4-dione (11). Shiny yellowish white micro crystals from ethanol, yield: 75% (0.78 g), mp: 197–199 °C, ^1H NMR (500 MHz, DMSO- d_6) δ : 8.47 (s, 1H, C $_4$ -H of quinoline), 7.92–7.85 (m, 2H, C $_{5,8}$ -H of quinoline), 7.57 (d, J = 3.0 Hz, 1H ArH), 7.45–7.43 (m, 1H, ArH), 7.34–7.31 (m, 3H, ArH), 7.28–7.2 (m, 1H, C $_5$ -H of quinoline), 6.32 (s, 1H, NH, D $_2$ O exchangeable), 4.64–4.60 (m, 1H, olefinic CH=C), 4.55–4.52 (m, 2H, CH $_2$), 3.89 (s, 3H, OCH $_3$); ^{13}C NMR (125 MHz, DMSO- d_6) δ : 172.6, 158.1, 157.7, 144.9, 142.7, 137.6, 136.8, 133.0, 129.1, 128.8, 128.7, 127.5, 127.2, 123.2, 106.5, 67.7, 56.0. Anal. Calcd. for C $_{21}$ H $_{16}$ ClN $_3$ O $_3$: C, 64.05; H, 4.09; N, 10.67. Found: C, 64.28; H, 4.42; N 11.03.

4.1.1.1.4. (Z)-3-benzyl-5-((2-chloro-7-methylquinolin-3-yl)methylene)imidazolidine-2,4-dione (12). Pale brown micro crystals from ethanol, yield: 38% (0.38 g), mp: 218–220 °C, ^1H NMR (500 MHz, DMSO- d_6) δ : 11.26 (s, 1H, NH, D $_2$ O exchangeable), 8.45 (s, 1H, C $_4$ -H of quinoline), 7.98–7.95 (m, 2H C $_{5,8}$ -H of quinoline), 7.75 (s, 1H, C $_6$ -H of quinoline), 7.32–7.24 (m, 5H, ArH), 6.71 (s, 1H, olefinic CH=C), 4.69–4.46 (m, 2H, CH $_2$), 2.49 (s, 3H, CH $_3$); ^{13}C NMR (125 MHz, DMSO- d_6) δ : 172.3 (C=O), 170.9, 157.4, 147.5, 146.8, 140.9, 138.4, 136.6, 130.9, 128.3, 128.2, 127.5, 127.0, 126.8, 124.8, 60.2, 21.4. Anal. Calcd. for

C $_{21}$ H $_{16}$ ClN $_3$ O $_2$: C, 66.76; H, 4.27; N, 11.12. Found: C, 66.88; H, 4.39; N 11.06.

4.1.1.1.5. (Z)-3-benzyl-5-((2-chloro-8-methylquinolin-3-yl)methylene)imidazolidine-2,4-dione (13). Yellow micro crystals from ethanol, yield: 45% (0.45 g), mp: 242–244 °C, ^1H NMR (500 MHz, DMSO- d_6) δ : 11.09 (s, 1H, NH, D $_2$ O exchangeable), 8.36 (s, 1H, C $_4$ -H of quinoline), 7.91–7.85 (m, 1H, C $_5$ -H of quinoline), 7.68–7.63 (m, 1H, C $_7$ -H of quinoline), 7.59–7.48 (m, 1H, C $_6$ -H of quinoline), 7.38–7.17 (m, 5H, ArH), 6.73 (s, 1H, olefinic CH=C), 4.69 (s, 2H, CH $_2$), 2.60 (s, 3H, CH $_3$); ^{13}C NMR (125 MHz, DMSO- d_6) δ : 163.7, 158.7, 154.7, 144.7, 138.1, 136.5, 134.3, 130.0, 128.6, 127.6, 125.7, 123.9, 119.4, 105.9, 51.1, 17.2. Anal. Calcd. for C $_{21}$ H $_{16}$ ClN $_3$ O $_2$: C, 66.76; H, 4.27; N, 11.12. Found: C, 66.92; H, 4.48; N 11.34.

4.1.1.1.6. (Z)-5-((2-chloroquinolin-3-yl)methylene)-3-phenethylimidazolidine-2,4-dione (14). Yellow crystals from ethanol, yield: 54% (0.50 g), mp: 194–196 °C, ^1H NMR (500 MHz, DMSO- d_6) δ : 10.89 (s, 1H, NH, D $_2$ O exchangeable), 8.32 (s, 1H, C $_4$ -H of quinoline), 7.66 (d, J = 7.0 Hz, 2H, C $_{5,8}$ -H of quinoline), 7.54–7.50 (m, 2H, C $_{6,7}$ -H of quinoline), 7.32–7.19 (m, 5H, ArH), 6.61 (s, 1H, olefinic CH=C), 3.71 (t, 2H, CH $_2$), 2.91 (t, 2H, CH $_2$); ^{13}C NMR (125 MHz, DMSO- d_6) δ : 163.6, 161.0, 154.1, 139.8, 138.2, 138.1, 131.1, 128.6, 128.5, 128.3, 127.5, 126.5, 124.9, 122.5, 119.4, 115.1, 103.5, 33.2. Anal. Calcd. For C $_{21}$ H $_{16}$ ClN $_3$ O $_2$: C, 66.76; H, 4.27; N, 11.12. Found: C, 67.03; H, 4.66; N 11.52.

4.1.1.1.7. (Z)-5-((2-chloro-6-methylquinolin-3-yl)methylene)-3-phenethylimidazolidine-2,4-dione (15). Off white micro crystals from ethanol, yield: 44% (0.42 g), mp: 203–205 °C, IR: ν_{max} /cm $^{-1}$: 3106 (NH), 3028 (CH, aromatic), 2942, 2855 (CH, aliphatic), 1701 (C=O), 1592 (C=N), 1454 (C=C), 1133 (C-O), 702 (C-Cl); ^1H NMR (500 MHz, DMSO- d_6) δ : 8.42 (s, 1H, C $_4$ -H of quinoline), 7.89–7.85 (m, 2H, C $_{5,8}$ -H of quinoline), 7.65 (d, J = 8.5 Hz, 1H, C $_7$ -H of quinoline), 7.32–7.29 (m, 2H, ArH), 7.24–7.20 (m, 3H, ArH), 6.25 (s, 1H, NH, D $_2$ O exchangeable), 5.32 (s, 1H, olefinic CH=C), 3.60–3.55 (m, 2H, CH $_2$), 2.81 (t, J = 7.5, 8.0 Hz, 2H, CH $_2$), 2.53 (s, 3H, CH $_3$); ^{13}C NMR (125 MHz, DMSO- d_6) δ : 172.1, 157.3, 146.4, 145.1, 138.3, 137.7, 136.9, 132.7, 132.6, 128.6, 128.5, 127.2, 127.0, 126.4, 67.6, 60.2, 33.5, 21.1. Anal. Calcd. for C $_{22}$ H $_{18}$ ClN $_3$ O $_2$: C, 67.43; H, 4.63; N, 10.72. Found: C, 67.70; H, 4.87; N 11.09.

4.1.1.1.8. (Z)-5-((2-chloro-6-methoxyquinolin-3-yl)methylene)-3-phenethylimidazolidine-2,4-dione (16). White crystals from ethanol, yield: 68% (0.68 g), mp: 216–218 °C, IR: ν_{max} /cm $^{-1}$: 3409 (OH), 3105 (NH), 3032 (CH, aromatic), 2935, 2875 (CH, aliphatic), 1700 (C=O), 1626 (C=N), 1456 (C=C), 701 (C-Cl); ^1H NMR (500 MHz, DMSO- d_6) δ : 8.43 (s, 1H, C $_4$ -H of quinoline), 7.87–7.82 (m, 2H, C $_{7,8}$ -H of quinoline), 7.56 (s, 1H, ArH), 7.45–7.43 (m, 1H, ArH), 7.32–7.29 (m, 1H, ArH), 7.24–7.20 (m, 3H, 2ArH + C $_5$ -H of quinoline), 6.23 (s, 1H, NH, D $_2$ O exchangeable), 5.32 (s, 1H, olefinic CH=C), 3.90 (s, 3H, OCH $_3$), 3.59–3.55 (m, 2H, CH $_2$), 2.82 (t, J = 7.5, 8.0 Hz, 2H, CH $_2$); ^{13}C

NMR (125 MHz, DMSO- d_6) δ : 172.2 (C=O), 157.8 (C=O), 157.4, 144.6, 142.5, 138.3, 137.3, 132.8, 128.9, 128.7, 128.5, 126.4, 122.9, 106.3, 67.5, 60.2, 55.7. Anal. Calcd. for $C_{22}H_{18}ClN_3O_3$: C, 64.79; H, 4.45; N, 10.30. Found: C, 64.66; H, 4.62; N 11.43.

4.1.1.1.9. (Z)-5-((2-chloro-7-methylquinolin-3-yl)methylene)-3-phenethylimidazolidine-2,4-dione (**17**). Light brown micro crystals from ethanol, yield: 78% (0.75 g), mp: 206–208 °C. 1H NMR (500 MHz, DMSO- d_6) δ : 11.22 (s, 1H, NH, D_2O exchangeable), 8.38 (s, 1H, C₄-H of quinoline), 7.98–7.95 (m, 2H C_{5,6}-H of quinoline), 7.39 (s, 1H, C₈-H of quinoline), 7.31–7.19 (m, 5H, ArH), 6.61 (s, 1H, olefinic CH=C), 4.46–4.37 (m, 2H, CH₂), 2.99–2.83 (m, 2H, CH₂), 2.44 (s, 3H, CH₃); ^{13}C NMR (125 MHz, DMSO- d_6) δ : 160.8, 157.8, 149.1, 146.7, 140.2, 139.4, 135.1, 130.6, 130.2, 129.9, 128.6, 127.9, 127.5, 125.9, 122.4, 50.3, 42.9, 20.6. Anal. Calcd. for $C_{22}H_{18}ClN_3O_2$: C, 67.43; H, 4.63; N, 10.72. Found: C, 67.49; H, 4.77; N 11.02.

4.1.1.1.10. (Z)-5-((2-chloro-7-methoxyquinolin-3-yl)methylene)-3-phenethylimidazolidine-2,4-dione (**18**). Pale brown micro crystals from ethanol, yield: 36% (0.36 g), mp: 263–265 °C. 1H NMR (500 MHz, DMSO- d_6) δ : 10.81 (s, 1H, NH, D_2O exchangeable), 8.25 (s, 1H, C₄-H of quinoline), 7.57 (d, J = 9.0 Hz, 1H, C₅-H of quinoline), 7.30–7.27 (m, 2H, C_{6,8}-H of quinoline), 7.22–7.18 (m, 3H, ArH), 6.87–6.82 (m, 2H, ArH), 6.57 (s, 1H, olefinic CH=C), 3.82 (s, 3H, OCH₃), 3.71 (t, J = 7.0, 8.0 Hz, 2H, CH₂), 2.90 (t, J = 7.5, 7.5 Hz, 2H, CH₂); ^{13}C NMR (125 MHz, DMSO- d_6) δ : 172.3, 163.4, 157.4, 154.9, 148.2, 146.4, 145.6, 139.0, 138.8, 136.6, 135.2, 132.4, 128.6, 128.3, 127.5, 127.0, 126.4, 125.0, 103.1, 67.5, 60.5. Anal. Calcd. for $C_{22}H_{18}ClN_3O_3$: C, 64.79; H, 4.45; N, 10.30. Found: C, 64.33; H, 4.62; N 11.56.

4.1.1.1.11. (Z)-5-((2-chloro-7-isopropoxyquinolin-3-yl)methylene)-3-phenethylimidazolidine-2,4-dione (**19**). Fine yellow micro crystals from ethanol, mp: 186–188 °C, yield: 78% (0.83 g). 1H NMR (500 MHz, DMSO- d_6) δ : 10.95 (s, 1H, NH, D_2O exchangeable), 8.33 (s, 1H, C₄-H of quinoline), 7.82–7.81 (m, 1H, C₅-H of quinoline), 7.70 (d, J = 2.5 Hz, 1H, C₈-H of quinoline), 7.40 (dd, J = 2.5, 2.5 Hz, 1H, C₆-H of quinoline), 7.30–7.27 (m, 2H, ArH), 7.22–7.19 (m, 3H, ArH), 6.40 (s, 1H, olefinic CH=C), 3.73 (t, J = 7.0, 8.0 Hz, 2H, CH₂), 3.24 (s, 1H, isopropoxy CH), 2.92 (t, J = 8.0, 7.0 Hz, 2H, CH₂), 1.65–1.61 (m, 6H, isopropoxy 2CH₃). ^{13}C NMR (125 MHz, DMSO- d_6) δ : 162.8, 157.9, 159.6, 152.6, 146.8, 138.1, 137.5, 130.6, 128.6, 127.7, 125.6, 124.8, 105.9, 119.4, 105.9, 80.3, 50.4, 43.2, 22.2. Anal. Calcd. for $C_{24}H_{22}ClN_3O_3$: C, 66.13; H, 5.09; N, 9.64. Found: C, 66.45; H, 4.89; N 9.93.

4.1.1.1.12. (Z)-5-((2-chloro-8-methylquinolin-3-yl)methylene)-3-phenethylimidazolidine-2,4-dione (**20**). Fine lemon yellow micro crystals from ethanol, yield: 82% (0.79 g), mp: 260–262 °C. 1H NMR (500 MHz, DMSO- d_6) δ : 11.17 (s, 1H, NH, D_2O exchangeable), 8.64 (s, 1H, C₄-H of quinoline), 7.92–7.85 (m, 1H, C₅-H of quinoline), 7.69–7.48 (m, 2H, C_{6,7}-H of quinoline), 7.31–7.15 (m, 5H, ArH), 6.67 (s, 1H, olefinic CH=C), 3.75–3.71 (m, 2H, CH₂), 2.92 (t, J = 8.0, 7.0 Hz, 2H, CH₂), 2.65 (s, 3H, CH₃); ^{13}C NMR (125 MHz, DMSO- d_6) δ : 163.3, 158.7, 154.9, 148.2, 144.9, 138.8, 138.0, 135.4, 134.3, 131.3, 129.7, 128.6, 128.5, 127.4, 126.5, 124.8, 119.4, 102.5, 51.0, 17.2. Anal. Calcd. for $C_{22}H_{18}ClN_3O_2$: C, 67.43; H, 4.63; N, 10.72. Found: C, 67.72; H, 4.79; N 11.02.

4.1.1.1.13. (Z)-3-benzyl-5-((2-methoxyquinolin-3-yl)methylene)imidazolidine-2,4-dione (**21**). Dark yellow micro crystals from ethanol, yield: 68% (0.64 g), mp: 330–332 °C, IR: ν_{max}/cm^{-1} ; 3163 (NH), 3026 (CH, aromatic), 2958, 2906 (CH, aliphatic), 1639 (C=O), 1554 (C=N), 1437 (C=C), 1207 (C–O); 1H NMR (500 MHz, DMSO- d_6) δ : 11.04 (s, 1H, NH, D_2O exchangeable), 8.36 (s, 1H, C₄-H of quinoline), 7.66 (d, J = 7.0 Hz, 1H, C₈-H of quinoline), 7.51 (t, J = 7.6 Hz, 1H, C₅-H of quinoline), 7.34–7.22 (m, 7H, C_{6,7}-H of quinoline + 5ArH), 6.67 (s, 1H, olefinic CH=C), 4.66 (s, 2H, CH₂), 3.68 (s, 3H, OCH₃); ^{13}C NMR (125 MHz, DMSO- d_6) δ : 163.8, 161.1, 154.4, 139.9, 138.2, 136.5, 131.1, 128.6, 128.4, 127.5, 127.4, 125.0, 122.5, 119.5, 115.1, 103.8, 41.4. Anal. Calcd. for $C_{21}H_{17}N_3O_3$: C, 70.18; H, 4.77; N, 11.69. Found: C, 70.37; H, 4.48; N 11.77.

4.1.1.1.14. (Z)-3-benzyl-5-((2,6-dimethoxyquinolin-3-yl)methylene)imidazolidine-2,4-dione (**22**). Pale brown crystals from ethanol, yield: 49% (0.50 g), mp: 172–174 °C, 1H NMR (500 MHz, DMSO- d_6) δ : 11.09 (s, 1H, NH, D_2O exchangeable), 8.47 (s, 1H, C₄-H of quinoline), 7.67 (d, J = 9.5 Hz, 1H, C₈-H of quinoline), 7.37–7.25 (m, 7H, C_{5,7}-H of quinoline + 5ArH), 6.72 (s, 1H, olefinic CH=C), 4.69 (s, 2H, CH₂), 4.00 (s, 3H, OCH₃), 3.86 (s, 3H, OCH₃); ^{13}C NMR (125 MHz, DMSO- d_6) δ : 163.6, 157.7, 155.8, 154.9, 140.5, 136.7, 136.4, 128.6, 128.4, 127.8, 127.5, 127.4, 125.4, 121.8, 117.4, 106.7, 102.2, 55.3, 53.6, 41.4. Anal. Calcd. for $C_{22}H_{19}N_3O_4$: C, 67.86; H, 4.92; N, 10.79. Found: C, 67.96; H, 5.09; N 10.99.

4.1.1.1.15. (Z)-5-((2-methoxyquinolin-3-yl)methylene)-3-phenethylimidazolidine-2,4-dione (**23**). Yellowish brown micro crystals from DMF, yield: 46% (0.42 g), mp: 315–317 °C, IR: ν_{max}/cm^{-1} ; 3170 (NH), 3022 (CH, aromatic), 2955, 2895 (CH, aliphatic), 1640 (C=O), 1559 (C=N), 1449 (C=C), 1213 (C–O); 1H NMR (500 MHz, DMSO- d_6) δ : 10.91 (s, 1H, NH, D_2O exchangeable), 8.38 (s, 1H, C₄-H of quinoline), 7.67 (d, J = 7.2 Hz, 1H, C₈-H of quinoline), 7.53 (t, J = 6.0, 7.6 Hz, 1H, C₅-H of quinoline), 7.35–7.24 (m, 7H, C_{6,7}-H of quinoline + 5ArH), 6.61 (s, 1H, olefinic CH=C), 3.74 (t, J = 7.8 Hz, 2H, CH₂), 3.34 (s, 3H, OCH₃), 2.94 (t, 2H, CH₂); ^{13}C NMR (125 MHz, DMSO- d_6) δ : 164.3, 161.1, 139.1, 139.0, 138.2, 137.9, 130.7, 128.6, 128.4, 128.1, 126.4, 125.4, 122.4, 119.6, 115.0, 102.3, 33.3. Anal. Calcd. for $C_{22}H_{19}N_3O_3$: C, 70.76; H, 5.13; N, 11.25. Found: C, 70.50; H, 4.88; N 11.37.

4.1.1.1.16. (Z)-5-((2,6-dimethoxyquinolin-3-yl)methylene)-3-phenethylimidazolidine-2,4-dione (**24**). Yellowish white crystals from ethanol, yield: 52% (0.52 g), mp: 185–187 °C, 1H NMR (400 MHz, DMSO- d_6) δ : 10.96 (s, 1H, NH, D_2O exchangeable), 8.46 (s, 1H, C₄-H of quinoline), 8.19 (d, J = 14.0 Hz, 1H C₈-H of quinoline), 7.75–7.67 (m, 2H, C_{5,7}-H of quinoline), 7.33–7.16 (m, 5H, ArH), 6.66 (s, 1H, olefinic CH=C), 4.02–3.98 (m, 2H, CH₂), 3.87 (s, 3H, OCH₃), 3.86 (s, 3H, OCH₃), 2.85–2.81 (m, 2H, CH₂); ^{13}C NMR (125 MHz, DMSO- d_6) δ : 172.5, 157.3, 155.7, 140.4, 138.3, 136.5, 135.7, 128.6, 128.4, 127.6, 126.4, 125.9, 125.5, 120.5, 107.0, 65.9, 60.2, 55.4, 53.3. Anal. Calcd. for $C_{23}H_{21}N_3O_4$: C, 68.47; H, 5.25; N, 10.42. Found: C, 68.65; H, 4.96; N 10.74.

4.1.1.1.17. (Z)-3-benzyl-5-((naphthalen-1-yl)methylene)imidazolidine-2,4-dione (**25**). White crystals from ethanol, yield: 72% (0.62 g), mp: 210–212 °C, IR: ν_{max}/cm^{-1} ; 3428 (OH), 3212 (NH), 3036 (CH, aromatic), 2924 (CH, aliphatic), 1672 (C=O), 1442 (C=C), 1156 (C–O); 1H NMR (500 MHz, DMSO- d_6) δ : 10.92 (s, 1H, NH, D_2O exchangeable), 8.07 (d, J = 8.0 Hz, 1H, C₅-H of naphthyl), 7.99–7.93 (m, 2H, C_{4,8}-H of naphthyl), 7.74 (d, J = 7.5 Hz, 1H, C₂-H of naphthyl), 7.62–7.54 (m, 3H, C_{3,6,7}-H of naphthyl), 7.38–7.29 (m, 5H, ArH), 7.14 (s, 1H, olefinic CH=C), 4.70 (s, 2H, CH₂); ^{13}C NMR (125 MHz, DMSO- d_6) δ : 163.6, 154.9, 136.5, 133.2, 131.0, 129.2, 129.0, 128.8, 128.7, 128.6, 127.5, 126.9, 126.3, 125.7, 123.7, 106.3, 41.4. Anal. Calcd. for $C_{21}H_{16}N_2O_2$: C, 76.81; H, 4.91; N, 8.53. Found: C, 77.06; H, 4.76; N 8.87.

4.1.1.1.18. (Z)-5-((naphthalen-1-yl)methylene)-3-phenethylimidazolidine-2,4-dione (**26**). Fine yellow micro crystals from ethanol, yield: 52% (0.44 g), mp: 170–172 °C, IR: ν_{max}/cm^{-1} ; 3466 (OH), 3265 (NH), 3028 (CH, aromatic), 2939 (CH, aliphatic), 1659 (C=O), 1505 (C=N), 1451 (C=C), 1155 (C–O); 1H NMR (400 MHz, DMSO- d_6) δ : 10.78 (s, 1H, NH, D_2O exchangeable), 8.07–7.23 (m, 12H, ArH), 7.09 (s, 1H, olefinic CH=C), 3.75 (t, J = 6.8, 6.4 Hz, 2H, CH₂), 2.95 (t, J = 6.4 Hz, 2H, CH₂); ^{13}C NMR (125 MHz, DMSO- d_6) δ : 163.6, 154.9, 138.1, 133.2, 131.0, 129.2, 128.9, 128.6, 128.5, 127.4, 126.9, 126.5, 126.3, 125.7, 123.6, 105.7, 67.3, 61.7. Anal. Calcd. for $C_{22}H_{18}N_2O_2$: C, 77.17; H, 5.30; N, 8.18. Found: C, 77.27; H, 5.48; N 8.33.

4.2. Biological evaluation

4.2.1. HIV-1 inhibitory activity

The inhibitory activity of compounds on HIV-1_{IIIB} replication in MT-2 cells was determined at Department of Biochemistry and Molecular

Biology, Drexel University, College of Medicine, Philadelphia, Pennsylvania 19102 United States as previously described [27]. See Appendix A.

4.2.2. Detection of *in vitro* cytotoxicity

The *in vitro* cytotoxicity of compounds on MT-2 cells was measured by XTT assay as previously described [28]. See Appendix A.

4.3. Docking study

In the preparation of the HIV-1 gp41 protein for docking, all CHR residues were removed except Trp631 and Asp632 amino acids which were reported to have important role in formation of 6-HB [21]. The ligand [29,30] and core structure of HIV-1 gp41 was prepared according to the previous report [31]. The grid parameters and docking parameters were prepared following the previously reported procedures [32–37].

Acknowledgment

This project was funded by the Deanship of Scientific Research (DSR), King Abdulaziz University, Jeddah, under Grant No. (RG-8-166-41). The authors, therefore, gratefully acknowledge DSR technical and financial support.

Declaration of Competing Interest

The authors declare no conflict of interest

Appendix A. Supplementary material

Supplementary data to this article can be found online at <https://doi.org/10.1016/j.bioorg.2020.103782>.

References

- [1] AIDS Epidemic Update UNAIDS (<http://www.unaids.org>), 2009.
- [2] V.A. Johnson, F. Brun-Vezinet, B. Clotet, B. Conway, R.T. D'Aquila, L.M. Demeter, D.R. Kuritzkes, D. Pillay, J.M. Schapiro, A. Telenti, D.D. Richman, Drug resistance mutations in HIV-1, *Top. HIV Med.* 11 (2003) 215–221.
- [3] D.D. Richman, S.C. Morton, T. Wrin, N. Hellmann, S. Berry, M.F. Shapiro, S.A. Bozzette, The prevalence of antiretroviral drug resistance in the United States, *AIDS* 18 (2004) 1393–1401.
- [4] A. Carr, D.A. Cooper, Adverse effects of antiretroviral therapy, *Lancet* 356 (2000) 1423–1430.
- [5] P. Yves, A.J. Allison, M. Christophe, *Nat. Rev. Drug Disc.* 4 (2005) 236.
- [6] C.B. Wilen, J.C. Tilton, R.W. Doms, HIV: cell binding and entry, *Cold Spring Harbor Perspect. Med.* 2 (2012).
- [7] M. Caffrey, HIV envelope: challenges and opportunities for development of entry inhibitors, *Trends Microbiol.* 19 (2011) 191–197.
- [8] C.A. Didigu, R.W. Doms, Novel approaches to inhibit HIV entry, *Viruses* 4 (2012) 309–324.
- [9] F. Yu, L. Lu, L. Du, X. Zhu, A.K. Debnath, S. Jiang, Approaches for identification of HIV-1 entry inhibitors targeting gp41 pocket, *Viruses* 5 (2013) 127–149.
- [10] L. Lu, F. Yu, L. Cai, A.K. Debnath, S. Jiang, Development of small-molecule HIV entry inhibitors specifically targeting gp120 or gp41, *Curr. Top. Med. Chem.* 16 (2016) 1074–1090.
- [11] D.M. Eckert, P.S. Kim, Mechanisms of viral membrane fusion and its inhibition, *Annu. Rev. Biochem.* 70 (2001) 777–810.
- [12] J.P. Moore, R.W. Doms, The entry of entry inhibitors: a fusion of science and medicine, *Proc. Natl. Acad. Sci. U.S.A.* 100 (2003) 10598–10602.
- [13] S. Liu, S. Wu, S. Jiang, HIV entry inhibitors targeting gp41: from polypeptides to small-molecule compounds, *Curr. Pharm. Des.* 13 (2007) 143–162.
- [14] M. Lu, S.C. Blacklow, P.S. Kim, A trimeric structural domain of the HIV-1 trans-membrane glycoprotein, *Nat. Struct. Biol.* 2 (1995) 1075–1082.
- [15] D.C. Chan, D. Fass, J.M. Berger, P.S. Kim, Core structure of gp41 from the HIV envelope glycoprotein, *Cell* 89 (1997) 263–273.
- [16] W. Weissenhorn, A. Dessen, S.C. Harrison, J.J. Skehel, D.C. Wiley, Atomic structure of the ectodomain from HIV-1 gp41, *Nature* 387 (1997) 426–428.
- [17] K. Tan, J. Liu, J.-H. Wang, S. Shen, M. Liu, Atomic structure of a thermostable subdomain of HIV-1 gp41, *Proc. Natl. Acad. Sci. U.S.A.* 94 (1997) 12303–12308.
- [18] D.C. Chan, C.T. Chutkowski, P.S. Kim, Evidence that a prominent cavity in the coiled coil of HIV type 1 gp41 is an attractive drug target, *Proc. Natl. Acad. Sci. U.S.A.* 95 (1998) 15613–15617.
- [19] S. Jiang, H. Lu, S. Liu, Q. Zhao, Y. He, A.K. Debnath, N-substituted pyrrole derivatives as novel human immunodeficiency virus type 1 entry inhibitors that interfere with the gp41 six-helix bundle formation and block virus fusion, *Antimicrob. Agents Chemother.* 48 (2004) 4349–4359.
- [20] A.R. Katritzky, S.R. Tala, H. Lu, A.V. Vakulenko, Q.Y. Chen, J. Sivapackiam, K. Pandya, S. Jiang, A.K. Debnath, Design, synthesis and structure-activity relationship of a novel series of 2-aryl 5-(4-oxo-3-phenethyl-2-thioxo-thiazolidinylidenemethyl) furans as HIV-1 entry inhibitors, *J. Med. Chem.* 52 (2009) 7631–7639.
- [21] S. Jiang, S.R. Tala, H. Lu, N.E. Abo-Dya, I. Avan, K. Gyanda, L. Lu, A.R. Katritzky, A.K. Debnath, Design, synthesis, and biological activity of novel 5-((arylfuran/1H-pyrrol-2-yl)methylene)-2-thioxo-3-(3-(trifluoromethyl)phenyl)thiazolidin-4-ones as HIV-1 fusion inhibitors targeting gp41, *J. Med. Chem.* 54 (2011) 572–579.
- [22] S. Jiang, S.R. Tala, H. Lu, P. Zou, I. Avan, T.S. Ibrahim, N.E. Abo-Dya, A. Abdelmajid, A.K. Debnath, A.R. Katritzky, Design, synthesis and biological activity of a novel series of 2,5-disubstituted furans/pyrroles as HIV-1 fusion inhibitors targeting gp41, *Bioorg. Med. Chem. Lett.* 21 (2011) 6895–6898.
- [23] G. Frey, S. Rits-Volloch, X.Q. Zhang, R.T. Schooley, B. Chen, S.C. Harrison, Small molecules that bind the inner core of gp41 and inhibit HIV envelope-mediated fusion, *Proc. Natl. Acad. Sci. U. S. A.* 103 (2006) 13938–13943.
- [24] S. Sardari, K. Azadmanesh, F. Mahboudi, A. Davood, R. Vahabpour, R. Zabiollahi, H. Gomari, Design of small molecules with HIV fusion inhibitory property based on Gp41 interaction assay, *Avicenna J. Med. Biotechnol.* 5 (2013) 78–86.
- [25] A. Srivastava, R.M. Singh, Vilsmeier-Haack reagent: A facile synthesis of 2-chloro-3-formyl quinolones from N-aryl acetamides and transformation into different functionalities, *Indian J. Chem.* 44B (2005) 1868–1875.
- [26] R.N. Comber, R.C. Reynolds, J.D. Friedrich, R.A. Manguikian, R.W. Buckheit, J.J.W. Truss, W.M. Shann, J.A. Secrist, 5,5-Di substituted Hydantoins and anti-HIV activity, *J. Med. Chem.* 35 (1992) 3567–3572.
- [27] C.A. Lipinski, F. Lombardo, B.W. Dominy, P.J. Feeney, Experimental and computational approaches to estimate solubility and permeability in drug discovery and development settings, *Adv. Drug Del. Rev.* 23 (1997) 3–25.
- [28] Q. Zhao, L. Ma, S. Jiang, H. Lu, S. Liu, Y. He, N. Strick, N. Neamati, A.K. Debnath, Identification of N-phenyl-N'-(2,2,6,6-tetramethyl-piperidin-4-yl)-oxalamides as a new class of HIV-1 entry inhibitors that prevent gp120 binding to CD4, *Virology* 339 (2005) 213–225.
- [29] H. Wang, Z. Qi, A. Guo, Q. Mao, H. Lu, X. An, C. Xia, X. Li, A.K. Debnath, S. Wu, S. Liu, S. Jiang, ADS-J1 inhibits human immunodeficiency virus type 1 entry by interacting with the gp41 pocket region and blocking fusion-active gp41 core formation, *Antimicrob. Agents Chemother.* 53 (2009) 4987–4998.
- [30] S. Sepehri, S. Soleymani, R. Zabiollahi, M.R. Aghasadeghi, M. Sadat, L. Saghale, A. Fassihi, Synthesis, biological evaluation, and molecular docking studies of Novel 4-[4-Arylpiperidin-1(4H)-yl]benzoic acid derivatives as Anti-HIV-1 agents, *Chem. Biodivers.* 1–14 (2017).
- [31] R. Munnaluri, S.K. Sivan, V. Manga, Molecular docking and MM/GBSA integrated protocol for designing small molecule inhibitors against HIV-1 gp41, *Med. Chem. Res.* 24 (2015) 829–841.
- [32] G.M. Morris, R. Huey, W. Lindstrom, M.F. Sanner, R.K. Belew, D.S. Goodsell, A.J. Olson, AutoDock4 and AutoDockTools4: Automated docking with selective receptor flexibility, *J. Comput. Chem.* 30 (2009) 2785–2791.
- [33] A.M. Gouda, F.A. Almalki, Carprofen: a theoretical mechanistic study to investigate the impact hydrophobic interactions of alkyl groups on modulation of COX – 1/2 binding selectivity, *SN Appl. Sci.* (2019), <https://doi.org/10.1007/s42452-019-0335-5>.
- [34] F.A. Almalki, A.M. Gouda, M.H. Bin Ali, O.M. Almeahmadi, Profens: a comparative molecular docking study into cyclooxygenase-1/2, *Drug Invent Today* 11 (2019) 480–487.
- [35] A.M. Shawky, M.A.S. Abourehab, A.N. Abdalla, A.M. Gouda, Optimization of pyrrolizine-based Schiff bases with 4-thiazolidinone motif: Design, synthesis and investigation of cytotoxicity and anti-inflammatory potency, *Eur. J. Med. Chem.* (2020), <https://doi.org/10.1016/j.ejmech.2019.111780>.
- [36] K.M. Attalah, A.N. Abdalla, A. Aslam, M. Ahmed, M.A.S. Abourehab, N.A. ElSawy, A.M. Gouda, Ethyl benzoate bearing pyrrolizine/indolizine moieties: Design, synthesis and biological evaluation of anti-inflammatory and cytotoxic activities, *Bioorg. Chem.* (2019), <https://doi.org/10.1016/j.bioorg.2019.103371>.
- [37] Dassault systems BIOVIA, Discovery Studio Visualizer, v16.1.0.15350, San Diego: Dassault systems, 2016.